Polarimetric MIMO Radar With Distributed Antennas for Target Detection

Sandeep Gogineni, *Student Member, IEEE*, and Arye Nehorai, *Fellow, IEEE*

***Abstract*—Multiple-input–multiple-output (MIMO) radar systems with widely separated antennas enable viewing the target from different angles, thereby providing spatial diversity gain. Polarimetric design of the transmit waveforms based on the properties of the target scattering matrix provides better performance than transmitting waveforms with only fixed horizontal or vertical polarizations. We propose a radar system that combines the advantages of both systems by transmitting polarized waveforms from multiple distributed antennas, in order to detect a point-like stationary target. The proposed system employs 2-D vector sensors at the receivers, each of which measures the horizontal and vertical components of the received electric field separately. We design the Neyman–Pearson detector for such systems. We derive approximate expressions for the probability of false alarm (P_{FA}) and the probability of detection (P_{D}). Using numerical simulations, we demonstrate that optimal design of the antenna polarizations provides improved performance over MIMO systems that transmit waveforms of fixed polarizations over all the antennas. We also demonstrate that having multiple widely separated antennas gives improved performance over single-input–single-output (SISO) polarimetric radar. We also demonstrate that processing the vector measurements at each receiver separately gives improved performance over systems that linearly combine both the received signals to give scalar measurements.**

***Index Terms*—Distributed, multiple-input–multiple-output (MIMO), polarimetric, radar.**

I. Introduction

THE polarization properties of any electromagnetic wave are usually altered when the wave reflects from the surface of a target. The target scattering matrix determines the change in polarization of the transmitted signal [1], [2]. Therefore, knowledge about the target in terms of its scattering matrix helps us design the optimal transmit waveform polarizations for performance improvement over systems transmitting waveforms with fixed polarizations over all the antennas. In [3]–[7], polarimetric design is suggested for use in conventional single antenna radar systems for problems such as detection, estimation and tracking. In [8], radar polarimetry is also used in multiple antenna systems with colocated antennas.

Manuscript received June 01, 2009; accepted October 12, 2009. First published November 10, 2009; current version published February 10, 2010. This work was supported by the Department of Defense under the Air Force Office of Scientific Research MURI Grant FA9550-05-1-0443 and ONR Grant N000140810849. The associate editor coordinating the review of this manuscript and approving it for publication was Dr. Biao Chen.

The authors are with the Department of Electrical and Systems Engineering, Washington University in St. Louis, St. Louis, MO 63130 USA (e-mail: sgogineni@ese.wustl.edu; nehorai@ese.wustl.edu).

Color versions of one or more of the figures in this paper are available online at http://ieeexplore.ieee.org.

Digital Object Identifier 10.1109/TSP.2009.2036472

In conventional single-antenna radar systems, the transmitter sends a signal in order to detect a target that reflects the signal towards the receiver [9]. The attenuation experienced by the signal depends on the properties of the target. In a realistic scenario, it is highly likely that the attenuation experienced will be a function of the angle of view of the target. If the angles of view of the target are sufficiently distinct from one another, then it is highly likely that the attenuation coefficients will have very little correlation. Therefore, even if some of the attenuation coefficients are extremely small, it is highly probable that they will be compensated by the others. Multiple-input–multiple-output (MIMO) radar with widely separated (distributed) antennas exploits this property by obtaining different views of the target [10], [11]. It employs multiple antennas to capture information from different angles, thereby exploiting the spatial diversity. Apart from this, MIMO radar has also been suggested for use in a colocated antenna configuration [12], [13]. Such a system exploits the flexibility of transmitting different waveforms from different elements of the array. Much work has been done on both (distributed and colocated) these configurations of MIMO radar recently because of the improvement in performance they offer [14]–[17].

In this paper we propose a radar system that combines the advantages of distributed-antenna MIMO systems with the advantages offered by optimally choosing the transmit waveform polarizations. We examine the problem of target detection for point targets. For each transmitter-receiver pair, a separate target scattering matrix specifies the attenuations across the different polarization pairs. Just as mentioned earlier, the correlation among the target scattering matrices becomes smaller if we have very widely spaced antennas that view the target from different angles. Therefore, these systems offer both spatial and polarization diversities. Vector sensors provide significant improvement in performance over scalar sensors for a variety of applications [18], [19]. Therefore, we use 2-D vector sensors to measure both the horizontal and vertical components of the electric field at each of the receivers in our proposed system. Most of the conventional polarimetric radar systems linearly and coherently combine the two received signals to give only a scalar measurement that depends on the receive polarization vector [2], [20]. This receive polarization vector is optimally chosen along with the transmit waveform polarizations in order to obtain improved performance [20]. However, we retain the received signals as vectors and demonstrate the advantages of doing so.

In Section II, we describe in detail the signal model for the proposed polarimetric MIMO radar system. We show that a linear model describes the measurements at the receivers. Later, in Section III, we formulate the radar target detection problem for this system. In Section IV, we present the Neyman–Pearson detector for this problem and derive the approximate analytical

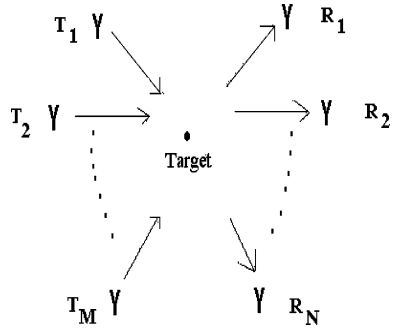

Fig. 1. MIMO radar system with widely separated antennas.

expressions for calculating the probability of detection (P_{D}) and the probability of false alarm (P_{FA}) of this detector under the given model. These results are important for choosing the optimal polarizations and also for analyzing the performance of the detector. For any fixed probability of false alarm, we find the optimal design by choosing the transmit polarizations that give the maximum probability of detection. In Section V, we develop a similar observation model for polarimetric radar systems that combine the two received signals to give only a scalar measurement. We present numerical results in Section VI, demonstrating the improvement in performance achieved by using the optimal transmit polarization vectors for a MIMO radar system with two transmit antennas and two receive antennas. We plot the receiver operating characteristic (ROC) curves of the optimal system, and also systems using either horizontal or vertical polarizations across all transmit antennas. We also have curves showing how the improvement in performance varies as a function of the noise variance. We also plot the ROC curves for polarimetric SISO radar to demonstrate the advantages of employing multiple widely separated antennas. We use numerical results to demonstrate the advantages of retaining the 2-D vector measurements at the receivers in our proposed system instead of combining them. Finally, we summarize our work in Section VII.

II. Signal Model

Before we develop the mathematical model, we describe the target and the radar system. We assume that the target is stationary and is present in the illuminated space. The target is further assumed to be point-like with a scattering matrix that depends on the angle of view. We consider a radar system that has M transmit antennas and N receive antennas with all the antennas widely spaced as shown in Fig. 1. Each of the receive antennas employs a 2-D vector sensor that measures both the horizontal and vertical components of the received polarized signal separately. Polarimetric models exist for describing the signals received in single-antenna systems [1], [2]. We extend these models to distributed antenna systems in this section.

We begin by describing the signals on the transmitter side. Define the polarization vector for the ith transmitter to be $\boldsymbol{t}^i = [t^i_{\mathrm{h}}, t^i_{\mathrm{v}}]^T$, where each of the entries of the polarization vectors is a complex number and $[\cdot]^T$ represents the transpose of $[\cdot]$. We further assume that $||\boldsymbol{t}^i|| = 1,\ \forall i = 1, \ldots, M$. The complex pulse wave shape transmitted from the ith transmit antenna is defined as $w^i(t)$. We assume that all these transmit waveforms are orthonormal to each other for all mutual delays between them [10], [11]. In other words, we assume that the cross correlation among these different waveforms is negligible for different lags. At the receiver side, this condition helps us differentiate between the signals transmitted from different transmit antennas.

After transmission, the polarized waveforms will travel in space and reflect off the surface of the target towards the receivers with altered polarimetric properties. We now consider the measurements on the receiver side. The polarized signal reaching the jth receive antenna is a combination of all the signals reflecting from the surface of the target towards the jth receiver. Let $\boldsymbol{y}^j(t)$ be the complex envelope of the signal received by the jth receive antenna. Note that $\boldsymbol{y}^j(t)$ is a 2-D column vector consisting of the horizontal and the vertical components of the received signal, and it is expressed using a formulation similar to that presented in [20]–[22]

$$\boldsymbol{y}^j(t) = \sum_{i=1}^{M} a^{ij} \boldsymbol{S}^{ij} \boldsymbol{t}^i w^i(t - \tau^{ij}) + \boldsymbol{e}^j(t) \tag{1}$$

where $\boldsymbol{e}^j(t)$ is the 2-D additive noise, τ^{ij} is the time delay because of propagation and the attenuation is divided into two factors a^{ij} and $\boldsymbol{S}^{ij}$. a^{ij} is that part of attenuation which depends on the properties of the medium, distance between the target and radar, etc. We assume that the coefficients $\{a^{ij}\}$ are known because the radar has an idea about the region which it is illuminating and the properties of the medium. $\boldsymbol{S}^{ij}$ represents the scattering matrix of the target, which completely describes the change in the polarimetric properties of the signal transmitted from the ith transmit antenna to the jth receive antenna. This represents the unknown part of the attenuation. It has four complex components and is given as

$$\boldsymbol{S}^{ij} = \begin{bmatrix} s^{ij}_{\mathrm{hh}} & s^{ij}_{\mathrm{hv}} \\ s^{ij}_{\mathrm{vh}} & s^{ij}_{\mathrm{vv}} \end{bmatrix}. \tag{2}$$

In order to separate the signals coming from different transmit antennas, the received signal is processed using a series of M matched filters at each receiver. At each receiver, the ith matched filter corresponds to a matching with the ith transmit waveform. We derive the mathematical model for the proposed MIMO radar system by using an approach similar to that presented for the single antenna system in [20]. The signals at the output of the matched filters are normalized by dividing by a^{ij}. Note that normalization changes the variances of the normalized noise term, and hence these variances need not be the same for all transmitter-receiver pairs. The normalized vector output of the ith matched filter at the jth receiver is expressed as

$$\boldsymbol{y}^{ij} = \boldsymbol{S}^{ij} \boldsymbol{t}^i + \boldsymbol{e}^{ij} \tag{3}$$

where the column vector $\boldsymbol{y}^{ij} = [y^{ij}_{\mathrm{h}}, y^{ij}_{\mathrm{v}}]^T$ consists of the horizontal and vertical components, respectively. We have now obtained the expressions for the measurements at each of the antennas on the receiver side. Next we perform some simple operations to express all these measurements using a linear model.

Stacking the elements of the scattering matrix $\boldsymbol{S}^{ij}$ into a vector, we define $\boldsymbol{s}^{ij} = [s^{ij}_{\mathrm{hh}}, s^{ij}_{\mathrm{hv}}, s^{ij}_{\mathrm{vh}}, s^{ij}_{\mathrm{vv}}]^T$. There are MN

such vectors, and arranging them into a single vector gives us a $4MN\times$ 1-D column vector:

$$\boldsymbol{s}=\left[(\boldsymbol{s}^{11})^T,\ldots,(\boldsymbol{s}^{1N})^T,\ldots,(\boldsymbol{s}^{M1})^T,\ldots,(\boldsymbol{s}^{MN})^T\right]^T. \quad (4)$$

Similarly, stacking the normalized outputs of the matched filters and also the corresponding additive noise components into column vectors, we define

$$\boldsymbol{y}=\left[(\boldsymbol{y}^{11})^T,\ldots,(\boldsymbol{y}^{1N})^T,\ldots,(\boldsymbol{y}^{M1})^T,\ldots,(\boldsymbol{y}^{MN})^T\right]^T \quad (5)$$

$$\boldsymbol{e}=\left[(\boldsymbol{e}^{11})^T,\ldots,(\boldsymbol{e}^{1N})^T,\ldots,(\boldsymbol{e}^{M1})^T,\ldots,(\boldsymbol{e}^{MN})^T\right]^T. \quad (6)$$

Define a set of matrices

$$\boldsymbol{P}^i=\begin{bmatrix} t_{\mathrm{h}}^i & t_{\mathrm{v}}^i & 0 & 0\\ 0 & 0 & t_{\mathrm{h}}^i & t_{\mathrm{v}}^i\end{bmatrix} \quad (7)$$

$\forall i=1,\ldots,M$, each corresponding to a particular transmit antenna.

Using the above definitions, we express the measurement vector $\boldsymbol{y}$ using the following mathematical model:

$$\boldsymbol{y}=\boldsymbol{H}\boldsymbol{s}+\boldsymbol{e} \quad (8)$$

where

$$\boldsymbol{H}=\begin{bmatrix} \boldsymbol{P}^1 & \ldots & \mathbf{0} & \ldots & \mathbf{0} & \ldots & \mathbf{0}\\ \vdots & \ddots & \vdots & \vdots & \vdots & \vdots & \vdots\\ \mathbf{0} & \ldots & \boldsymbol{P}^1 & \ldots & \mathbf{0} & \ldots & \mathbf{0}\\ \vdots & \vdots & \vdots & \ddots & \vdots & \vdots & \vdots\\ \mathbf{0} & \ldots & \mathbf{0} & \ldots & \boldsymbol{P}^M & \ldots & \mathbf{0}\\ \vdots & \vdots & \vdots & \vdots & \vdots & \ddots & \vdots\\ \mathbf{0} & \ldots & \mathbf{0} & \ldots & \mathbf{0} & \ldots & \boldsymbol{P}^M\end{bmatrix}. \quad (9)$$

$\mathbf{0}$ is a zero matrix of dimensions 2×4. Terms $\boldsymbol{y}$ and $\boldsymbol{e}$ are $2MN\times$ 1-D observation and noise vectors, respectively. Thus, we have reduced our mathematical model to the well-known linear form. We now look at the statistical assumptions made on these terms.

We assume that the noise terms present in $\boldsymbol{e}$ are uncorrelated and that $\boldsymbol{e}$ follows proper complex Gaussian distribution. A complex random vector $\varsigma=\varsigma_{\mathrm{R}}+j\varsigma_{\mathrm{I}}$ is said to be proper if $\mathrm{Cov}(\varsigma_{\mathrm{R}},\varsigma_{\mathrm{R}})=\mathrm{Cov}(\varsigma_{\mathrm{I}},\varsigma_{\mathrm{I}})$ and $\mathrm{Cov}(\varsigma_{\mathrm{R}},\varsigma_{\mathrm{I}})=-\mathrm{Cov}(\varsigma_{\mathrm{I}},\varsigma_{\mathrm{R}})$. Hence, the covariance matrix of $\boldsymbol{e}$ will be diagonal. This diagonal assumption states that the noise components at the outputs of the matched filters across the various widely separated receivers over both the polarizations are statistically independent for any given time snapshot. This assumption is reasonable given the wide separation between the antennas [10]. The diagonal entries of the covariance matrix of $\boldsymbol{e}$ need not be the same because of the normalization performed at the output of each of the matched filters, as mentioned earlier. Define this covariance matrix as $\boldsymbol{\Sigma_e}$ and assume that it is known. The matrix $\boldsymbol{H}$ is a $2MN\times 4MN$ dimensional design matrix whose constituent elements depend on the transmit waveform polarizations. We assume that the vector $\boldsymbol{s}$, which contains elements from all the scattering matrices, is a random vector following proper complex Gaussian distribution with a $4MN\times 4MN$ covariance matrix given by $\boldsymbol{\Sigma_s}$. We further assume that $\boldsymbol{\Sigma_s}$ is known. If the random matrices $\boldsymbol{S}^{ij}$ are statistically independent, then $\boldsymbol{\Sigma_s}$ will have a block diagonal structure. However, we do not impose any such structural constraint on $\boldsymbol{\Sigma_s}$. Furthermore, we assume that $\boldsymbol{s}$ and $\boldsymbol{e}$ are independent. Since we have described all the terms in our measurement model, we shall formally state the detection problem in Section III.

III. Problem Formulation

The above mathematical model gives an expression for the observation vector when the target is present in the illuminated space. When the target is absent, the observations will consist of only the receiver noise vector $\boldsymbol{e}$. Hence, the problem of detecting the target reduces to the following binary hypothesis testing problem:

$$H_0:\boldsymbol{y}=\boldsymbol{e} \quad (10)$$

$$H_1:\boldsymbol{y}=\boldsymbol{H}\boldsymbol{s}+\boldsymbol{e}. \quad (11)$$

Therefore, under the null hypothesis, $\boldsymbol{y}$ will have complex Gaussian distribution with zero mean and covariance matrix $\boldsymbol{\Sigma_e}$. Under the alternative hypothesis, the independence of $\boldsymbol{s}$ and $\boldsymbol{e}$ implies that $\boldsymbol{y}$ will follow complex Gaussian distribution with zero mean and covariance matrix given by $\boldsymbol{C}+\boldsymbol{\Sigma_e}$, where $\boldsymbol{C}=\boldsymbol{H}\boldsymbol{\Sigma_s}\boldsymbol{H}^H$ denotes the covariance matrix of $\boldsymbol{Hs}$. This result is an application of the well-known properties of Gaussian random vectors [23]. Next we describe the Neyman–Pearson detector for this problem.

IV. Detector

A. Test Statistic

Under the above-mentioned hypotheses, the probability density functions of the observation vector are given as

$$f(\boldsymbol{y}\,|\,H_0)\propto\frac{1}{|\boldsymbol{\Sigma_e}|}e^{-\boldsymbol{y}^H\boldsymbol{\Sigma_e}^{-1}\boldsymbol{y}} \quad (12)$$

$$f(\boldsymbol{y}\,|\,H_1)\propto\frac{1}{|\boldsymbol{\Sigma_e}+\boldsymbol{C}|}e^{-\boldsymbol{y}^H(\boldsymbol{\Sigma_e}+\boldsymbol{C})^{-1}\boldsymbol{y}}. \quad (13)$$

The Neyman–Pearson lemma states that the likelihood ratio test is the most powerful test for any given size [24]. The likelihood ratio is given as

$$\frac{f(\boldsymbol{y}\,|\,H_0)}{f(\boldsymbol{y}|H_1)}=\frac{|\boldsymbol{\Sigma_e}+\boldsymbol{C}|}{|\boldsymbol{\Sigma_e}|}e^{-\boldsymbol{y}^H(\boldsymbol{\Sigma_e}^{-1}-(\boldsymbol{\Sigma_e}+\boldsymbol{C})^{-1})\boldsymbol{y}}. \quad (14)$$

Computing the logarithm of the above expression and ignoring the known constants, we clearly see that $\boldsymbol{y}^H(\boldsymbol{\Sigma_e}^{-1}-(\boldsymbol{\Sigma_e}+\boldsymbol{C})^{-1})\boldsymbol{y}$ is our test statistic and we compare it with a threshold before selecting a hypothesis

$$\boldsymbol{y}^H(\boldsymbol{\Sigma_e}^{-1}-(\boldsymbol{\Sigma_e}+\boldsymbol{C})^{-1})\boldsymbol{y}\gtrless_{H_0}^{H_1}k \quad (15)$$

where the threshold k is chosen based on the size specified for the test.

B. Estimating Covariance Matrices

In practice, the covariance matrices needed for implementing the detector may not be known in advance. In such a scenario,

the maximum likelihood estimates (MLE) of these matrices can be substituted to perform the test. Since the observations follow Gaussian distribution under both the hypotheses, the MLE of the covariance matrices are given by the corresponding sample covariance matrices [24], [25]. The sample covariance matrices are easy to compute in practice. The variance of noise at each receiver is calculated before the detector starts functioning by evaluating the sample variance using a large set of training data. The covariance matrix under the alternative hypothesis is estimated by evaluating the sample covariance matrix using all the samples of observations in a particular window of time when the detector is in use. These two estimated matrices are sufficient for implementing the detector. If there is no target in the illuminated space, then these two estimated matrices will be close to each other, thereby causing the test statistic to fall below the threshold.

C. Performance Analysis

In order to analyze the performance of the above-mentioned detector, we need to know the distribution of the test statistic under both hypotheses. The test statistic is a quadratic form of the complex Gaussian random vector $\boldsymbol{y}$. It is well known in statistics that a quadratic form $\boldsymbol{z}^T\boldsymbol{U}\boldsymbol{z}$ of a real Gaussian random vector $\boldsymbol{z}$ with covariance matrix $\boldsymbol{B}$ will follow Chi-square distribution if and only if the matrix $\boldsymbol{U}B$ is idempotent [26]. Using this result, we infer that our test statistic does not necessarily follow Chi-square distribution for all feasible choices of $\boldsymbol{\Sigma_e}$ and $\boldsymbol{C}$ because we did not impose any constraint on $\boldsymbol{\Sigma_s}$. Hence, it is difficult to find the exact probability density function (pdf) for it. In order to study the pdf of our test statistic, we first begin with an assumption that $\boldsymbol{C}$ is diagonal. Later, we will extend this approach to the non-diagonal case by applying proper diagonalization.

Define the lth diagonal element of $\boldsymbol{C}$ as c^l and that of $\boldsymbol{\Sigma_e}$ as v^l. Then, the test statistic reduces to

$$\sum_{i=1}^{M}\sum_{j=1}^{N}\left(\frac{\left|y_{\mathrm{h}}^{ij}\right|^2}{v^{2(i-1)N+2j-1}} - \frac{\left|y_{\mathrm{h}}^{ij}\right|^2}{v^{2(i-1)N+2j-1}+c^{2(i-1)N+2j-1}}\right) + \sum_{i=1}^{M}\sum_{j=1}^{N}\left(\frac{\left|y_{\mathrm{v}}^{ij}\right|^2}{v^{2(i-1)N+2j}} - \frac{\left|y_{\mathrm{v}}^{ij}\right|^2}{v^{2(i-1)N+2j}+c^{2(i-1)N+2j}}\right)$$

where $y_{\mathrm{h}}^{ij}, y_{\mathrm{v}}^{ij}$ are always independent Gaussian random variables under both hypotheses for all transmitter-receiver pairs because of the diagonal assumption of $\boldsymbol{\Sigma_e}$ and $\boldsymbol{C}$. Therefore, the test statistic is a weighted sum of independent Chi-square random variables and it does not necessarily follow the Chi-square distribution. Its actual distribution depends on the weights. The pdf of a sum of independent random variables is obtained by performing multiple convolutions among the constituent pdfs. However, in this case, it is difficult to find the exact solution. Hence, we shall look for approximations to the actual pdf.

In [27], the distribution of the weighted sum of Chi squares is studied. If π_q are real positive constants and N_q are independent standard normal random variables $\forall q = 1, \ldots, K$, then the pdf of the Gamma approximation of $R = \sum_{q=1}^{K} \pi_q {N_q}^2$ is given as

$$f_R(r,\alpha,\beta) = r^{\alpha-1}\frac{e^{-\frac{r}{\beta}}}{\beta^{\alpha}\Gamma(\alpha)} \tag{16}$$

where the parameters α and β are given as

$$\alpha = \frac{1}{2}\left(\frac{\left(\sum_{q=1}^{K}\pi_q\right)^2}{\sum_{q=1}^{K}\pi_q^2}\right) \tag{17}$$

$$\beta = \left(\frac{1}{2}\left(\frac{\sum_{q=1}^{K}\pi_q}{\sum_{q=1}^{K}\pi_q^2}\right)\right)^{-1}. \tag{18}$$

Γ is the gamma function defined as $\Gamma(\alpha) = \int_0^{\infty} t^{\alpha-1}e^{-t}dt$.

Under the null hypothesis, y_{h}^{ij} and y_{v}^{ij} have zero mean and variances $v^{(2(i-1)N+2j-1)}$ and $v^{(2(i-1)N+2j)}$, respectively. Hence, applying the above approximation with appropriate weights, the parameters of the Gamma distribution are

$$\alpha_{H_0} = \left(\frac{\left(\sum_{l=1}^{2MN}\frac{c^l}{v^l+c^l}\right)^2}{\sum_{l=1}^{2MN}\left(\frac{c^l}{v^l+c^l}\right)^2}\right) \tag{19}$$

$$\beta_{H_0} = \left(\frac{\sum_{l=1}^{2MN}\frac{c^l}{v^l+c^l}}{\sum_{l=1}^{2MN}\left(\frac{c^l}{v^l+c^l}\right)^2}\right)^{-1}. \tag{20}$$

Under the alternative hypothesis, y_{h}^{ij} and y_{v}^{ij} have zero mean and variances $v^{(2(i-1)N+2j-1)} + c^{(2(i-1)N+2j-1)}$ and $v^{(2(i-1)N+2j)} + c^{(2(i-1)N+2j)}$, respectively. The parameters of the Gamma approximation are

$$\alpha_{H_1} = \left(\frac{\left(\sum_{l=1}^{2MN}\frac{c^l}{v^l}\right)^2}{\sum_{l=1}^{2MN}\left(\frac{c^l}{v^l}\right)^2}\right) \tag{21}$$

$$\beta_{H_1} = \left(\frac{\sum_{l=1}^{2MN}\frac{c^l}{v^l}}{\sum_{l=1}^{2MN}\left(\frac{c^l}{v^l}\right)^2}\right)^{-1}. \tag{22}$$

Note that so far we have assumed a diagonal structure for matrix $\boldsymbol{C}$ in the above discussion. However, we still need to find expressions for the pdf of the test statistic when $\boldsymbol{C}$ is not diagonal. Diagonalization will be used to extend the analysis even for the case of non-diagonal matrices [28]. Since $\boldsymbol{\Sigma_e}$ and $\boldsymbol{C}$ are covariance matrices, $(\boldsymbol{\Sigma_e}^{-1} - (\boldsymbol{\Sigma_e}+\boldsymbol{C})^{-1})$ will be a Hermitian matrix, which therefore decomposes into $\boldsymbol{D}^H\boldsymbol{\Lambda}\boldsymbol{D}$, where $\boldsymbol{\Lambda}$ is a diagonal matrix consisting of eigenvalues as the diagonal elements and $\boldsymbol{D}$ contains the corresponding orthonormal eigenvectors. The test statistic now becomes $(\boldsymbol{D}\boldsymbol{y})^H\boldsymbol{\Lambda}(\boldsymbol{D}\boldsymbol{y})$. If we show that $\boldsymbol{D}\boldsymbol{y}$ has a diagonal covariance matrix under both hypotheses, then our analysis extends to the case in which $\boldsymbol{C}$ is not diagonal also, with appropriate adjustments made to the parameters of the Gamma approximation. Under H_0, $\boldsymbol{D}\boldsymbol{y}$ is

a complex Gaussian random vector with a covariance matrix $\mathrm{Cov}_{H_0}(\boldsymbol{Dy}) = \boldsymbol{D\Sigma_e D}^H$, which is diagonal because $\boldsymbol{\Sigma_e}$ is diagonal and $\boldsymbol{D}$ has orthonormal vectors. Similarly, under H_1, $\boldsymbol{Dy}$ is a complex normal random vector with covariance matrix

$$\begin{aligned}\mathrm{Cov}_{H_1}(\boldsymbol{Dy}) &= \boldsymbol{D}(\boldsymbol{\Sigma_e}+\boldsymbol{C})\boldsymbol{D}^H \\ &= \left(\boldsymbol{D}(\boldsymbol{\Sigma_e}+\boldsymbol{C})^{-1}\boldsymbol{D}^H\right)^{-1} \\ &= \left(\boldsymbol{D}((\boldsymbol{\Sigma_e}+\boldsymbol{C})^{-1}-\boldsymbol{\Sigma_e}^{-1}+\boldsymbol{\Sigma_e}^{-1})\boldsymbol{D}^H\right)^{-1} \\ &= \left(\boldsymbol{D\Sigma_e}^{-1}\boldsymbol{D}^H-\boldsymbol{\Lambda}\right)^{-1}\end{aligned}$$

which is diagonal. Hence, under both hypotheses, the test statistic is a weighted sum of Chi square random variables even when matrix $\boldsymbol{C}$ is not diagonal. The only difference is that the weights will now be different, and they are defined by the diagonalization process.

After approximating the pdf using the Gamma density, the probability of detection (P_{D}) and the probability of false alarm (P_{FA}) are defined as follows:

$$P_{\mathrm{D}} = \int_k^\infty t^{\alpha_{H_1}-1}\frac{e^{-\frac{t}{\beta_{H_1}}}}{\beta_{H_1}^{\alpha_{H_1}}\Gamma(\alpha_{H_1})}dt \tag{23}$$

$$P_{\mathrm{FA}} = \int_k^\infty t^{\alpha_{H_0}-1}\frac{e^{-\frac{t}{\beta_{H_0}}}}{\beta_{H_0}^{\alpha_{H_0}}\Gamma(\alpha_{H_0})}dt \tag{24}$$

where the parameters $\alpha_{H_0}, \beta_{H_0}, \alpha_{H_1}$, and β_{H_1} are as mentioned earlier. For a given value of P_{FA}, the value of the threshold k is calculated easily using the above expression because functions for evaluating the above expressions exist in MATLAB. After finding the threshold, P_{D} is calculated accordingly. Note that the value of the threshold and P_{D} depends on matrix $\boldsymbol{C}$, which in turn depends on the polarizations of the transmitted waveforms. Hence, the performance of the detector is related to the transmit waveform polarizations.

D. Optimal Design

In order to find the optimal design, we perform a grid search over the possible waveform polarizations across all the transmit antennas with the help of the above expressions for P_{D} and P_{FA}. The optimal design corresponds to the transmit polarizations that give the maximum P_{D} for a given P_{FA}. Later, we will plot the ROC curves to visualize the improvement in performance because of the optimal design. We demonstrate this in Section VI with appropriate numerical examples.

V. Scalar Measurement Model

Most of the conventional polarimetric radar systems combine the two received signals linearly and coherently at each receiver to give only a scalar measurement that depends on the receive polarization vector. For such systems, the output at each receive antenna is modeled as an inner product of the received signal and the receive antenna polarization [2], [20]. This receive polarization vector is optimally chosen along with the transmit waveform polarizations in order to achieve improved performance. We now use a similar approach to that used in Section II in order to obtain the signal model for such systems. From now on, we refer to this model as the scalar measurement model.

Let $\boldsymbol{r}^j = [r_{\mathrm{h}}^j, r_{\mathrm{v}}^j]^T$ be the polarization vector of the jth receiver, where each of the entries is a complex number. We further assume that $\|\boldsymbol{r}^j\| = 1, \forall j = 1,\ldots,N$. The rest of the variables remain the same as defined earlier in Section II, except that the measurement and the noise at each receiver according to this model will be complex scalars. The scalar observation at the jth receiver $y^j(t)$ is now expressed as follows [20]–[22]:

$$y^j(t) = \sum_{i=1}^{M} a^{ij}\boldsymbol{r}^{jT}\boldsymbol{S}^{ij}\boldsymbol{t}^i w^i(t-\tau^{ij}) + e^j(t). \tag{25}$$

This signal is now passed through a series of matched filters whose outputs are appropriately normalized to move the effect of a^{ij} into the noise term. Finally, the normalized output of the ith matched filter at the jth receiver is given as

$$y^{ij} = \boldsymbol{r}^{jT}\boldsymbol{S}^{ij}\boldsymbol{t}^i + e^{ij}. \tag{26}$$

Stacking all the observations and the noise components into column vectors, in a similar fashion to the approach used in Section II, we obtain $MN\times$ 1-D vectors $\boldsymbol{y}$ and $\boldsymbol{e}$, respectively. Vector $\boldsymbol{s}$ remains the same as defined earlier. However, matrix $\boldsymbol{H}$ changes and now contains the elements of the receive polarization vectors also. Let us define a set of vectors

$$\boldsymbol{\eta}^{ij} = \left[\left(r_{\mathrm{h}}^j t_{\mathrm{h}}^i\right), \left(r_{\mathrm{h}}^j t_{\mathrm{v}}^i\right), \left(r_{\mathrm{v}}^j t_{\mathrm{h}}^i\right), \left(r_{\mathrm{v}}^j t_{\mathrm{v}}^i\right)\right] \tag{27}$$

$\forall i = 1,\ldots,M$, $j = 1,\ldots,N$ each of which corresponds to a particular transmitter-receiver pair. Under this definition, the observation vector is expressed as

$$\boldsymbol{y} = \boldsymbol{Hs} + \boldsymbol{e} \tag{28}$$

where $\boldsymbol{H}$ is a $MN \times 4MN$ dimensional matrix given by

$$\boldsymbol{H} = \begin{bmatrix} \boldsymbol{\eta}^{11} & \cdots & \mathbf{0} & \cdots & \mathbf{0} & \cdots & \mathbf{0} \\ \vdots & \ddots & \vdots & \vdots & \vdots & \vdots & \vdots \\ \mathbf{0} & \cdots & \boldsymbol{\eta}^{1N} & \cdots & \mathbf{0} & \cdots & \mathbf{0} \\ \vdots & \vdots & \vdots & \ddots & \vdots & \vdots & \vdots \\ \mathbf{0} & \cdots & \mathbf{0} & \cdots & \boldsymbol{\eta}^{M1} & \cdots & \mathbf{0} \\ \vdots & \vdots & \vdots & \vdots & \vdots & \ddots & \vdots \\ \mathbf{0} & \cdots & \mathbf{0} & \cdots & \mathbf{0} & \cdots & \boldsymbol{\eta}^{MN} \end{bmatrix}. \tag{29}$$

Therefore, we obtain a similar linear model even for the systems with scalar measurements. The only difference lies in the dimensionality of some of the vectors in the model and also the constituent elements of the matrix $\boldsymbol{H}$. The optimal design for such a system will not only include optimization over the transmit polarizations $\boldsymbol{t}^i$ but will also include the optimal selection of the receive polarization vectors $\boldsymbol{r}^j$. The problem formulation and analysis of the detector remains the same as for the earlier model because the basic structure of the model is still the same. Hence, the analysis performed in Section IV is applicable even to this model. We use this analysis in the next section to demonstrate the advantage of retaining the vector measurements at each receiver without combining them.

VI. Numerical Results

We consider a system with two transmit antennas and two receive antennas under the same target detection scenario as described so far. Hence, there are 16 complex elements in the random vector $\boldsymbol{s}$. We choose the covariance matrix of this vector to be of the following form:

$$\boldsymbol{\Sigma}_{\boldsymbol{s}} = \begin{bmatrix} \boldsymbol{\Sigma}_{\boldsymbol{s}}^{11} & \mathbf{0} & \mathbf{0} & \mathbf{0} \\ \mathbf{0} & \boldsymbol{\Sigma}_{\boldsymbol{s}}^{12} & \mathbf{0} & \mathbf{0} \\ \mathbf{0} & \mathbf{0} & \boldsymbol{\Sigma}_{\boldsymbol{s}}^{21} & \mathbf{0} \\ \mathbf{0} & \mathbf{0} & \mathbf{0} & \boldsymbol{\Sigma}_{\boldsymbol{s}}^{22} \end{bmatrix} \tag{30}$$

where $\boldsymbol{\Sigma}_{\boldsymbol{s}}^{ij}$ represents the covariance matrix of the random vector $\boldsymbol{s}^{ij}$ and $\mathbf{0}$ is a 4×4 dimensional zero matrix. Each of these matrices were chosen as follows:

$$\boldsymbol{\Sigma}_{\boldsymbol{s}}^{11} = \begin{bmatrix} 0.3 & 0.1\epsilon & 0.1\epsilon & 0.1\epsilon \\ 0.1\epsilon^* & 0.2 & 0.1\epsilon & 0.1\epsilon \\ 0.1\epsilon^* & 0.1\epsilon^* & 0.4 & 0.1\epsilon \\ 0.1\epsilon^* & 0.1\epsilon^* & 0.1\epsilon^* & 0.5 \end{bmatrix} \tag{31}$$

$$\boldsymbol{\Sigma}_{\boldsymbol{s}}^{12} = \begin{bmatrix} 0.5 & 0.05\epsilon & 0.05\epsilon & 0.05\epsilon \\ 0.05\epsilon^* & 0.3 & 0.05\epsilon & 0.05\epsilon \\ 0.05\epsilon^* & 0.05\epsilon^* & 0.4 & 0.05\epsilon \\ 0.05\epsilon^* & 0.05\epsilon^* & 0.05\epsilon^* & 0.3 \end{bmatrix} \tag{32}$$

$$\boldsymbol{\Sigma}_{\boldsymbol{s}}^{21} = \begin{bmatrix} 0.4 & 0.1\epsilon & 0.1\epsilon & 0.1\epsilon \\ 0.1\epsilon^* & 0.3 & 0.1\epsilon & 0.1\epsilon \\ 0.1\epsilon^* & 0.1\epsilon^* & 0.2 & 0.1\epsilon \\ 0.1\epsilon^* & 0.1\epsilon^* & 0.1\epsilon^* & 0.4 \end{bmatrix} \tag{33}$$

$$\boldsymbol{\Sigma}_{\boldsymbol{s}}^{22} = \begin{bmatrix} 0.4 & 0.05\epsilon & 0.05\epsilon & 0.05\epsilon \\ 0.05\epsilon^* & 0.4 & 0.05\epsilon & 0.05\epsilon \\ 0.05\epsilon^* & 0.05\epsilon^* & 0.2 & 0.05\epsilon \\ 0.05\epsilon^* & 0.05\epsilon^* & 0.05\epsilon^* & 0.5 \end{bmatrix} \tag{34}$$

where $\epsilon = 1+\sqrt{-1}$. The complex elements of the noise vector $\boldsymbol{e}$ are assumed to be uncorrelated, with the variance of each equal to $\sigma^2 = 0.2$. Before we use the Gamma approximation to obtain the optimal design, we first check if the approximation is reasonable, in our case by plotting the cumulative distribution function (cdf) of the approximate Gamma distribution and comparing it with that formed by generating random samples from the constituent Chi squares. This comparison assumes all the antennas are horizontally polarized.

In this scenario, we have the following information available:

$$\boldsymbol{t}^1 = [1, 0] \tag{35}$$

$$\boldsymbol{t}^2 = [1, 0]. \tag{36}$$

Therefore, the matrices $\boldsymbol{P}^1$ and $\boldsymbol{P}^2$ become $\boldsymbol{P}^1 = \boldsymbol{P}^2 = \begin{bmatrix} 1 & 0 & 0 & 0 \\ 0 & 0 & 1 & 0 \end{bmatrix}$. The matrix $\boldsymbol{C}$ turns out to be non-diagonal for this example. Hence, after performing the appropriate diagonalization and calculating the weights, the coefficients of the Gamma approximation under the null hypothesis turn out to be $\alpha_{H_0} = 7.6833$ and $\beta_{H_0} = 0.6283$. Fig. 2(b) shows the cdf of this approximated Gamma distribution with the above-mentioned parameters. In order to check if this is indeed a good approximation, we generated random samples of the observation vector $\boldsymbol{y}$ under the null hypothesis. We evaluated the test statistic $\boldsymbol{y}^H(\boldsymbol{\Sigma_e}^{-1} - (\boldsymbol{\Sigma_e} + \boldsymbol{C})^{-1})\boldsymbol{y}$ for each of these

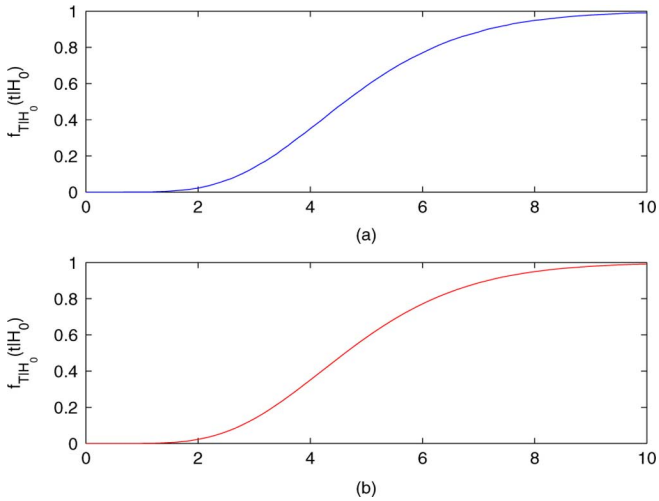

Fig. 2. Cumulative distribution function of the test statistic for the chosen example under the null hypothesis. (a) Sample cdf. (b) Gamma approximation.

random samples and generated the sample cumulative distribution function, which is plotted in Fig. 2(a). It is clear from both figures that the Gamma approximation we made is indeed very accurate and close to the sample distribution. This finding is consistent with the results presented in [27]. The sample cdf takes values 0.5827 and 0.9233 whereas the cdf of the Gamma approximation takes values 0.5863 and 0.9242 for argument values of 5 and 7.5, respectively. This shows that the values taken by these two curves differ only at the third decimal point.

Now that we have a good enough approximation to the distribution of our test statistic, we look at how the optimal choice of polarizations improves the performance of the detector. We fix the complex noise variance to $\sigma^2 = 0.2$ and vary the value of P_{FA}. This method enables us to plot the optimal ROC curve by performing a grid search using the analytical results derived earlier in the paper. Next, we obtain the reference curves for our results by computing the ROC curves assuming that all the transmit antennas are horizontally or vertically polarized. These plots are presented in Fig. 3, and a significant improvement in performance is clearly visible while using the optimal waveform polarizations.

We proceed with our analysis for this numerical example. First, we fix P_{FA} to be equal to 0.02. For this value of P_{FA}, we wish to check the improvement offered by the optimal design for different values of the noise variance. We plot the optimal P_{D} as a function of σ^2. We also plot P_{D} as a function of σ^2 for the case in which only horizontal or vertical polarizations are used. The improvement in performance offered by the optimal design is clear from Fig. 4.

So far, we have demonstrated that by optimally selecting the transmit polarizations, we get performance improvement over conventional MIMO systems with fixed polarizations. Now, we plot the ROC curves for SISO radar with optimal transmit polarizations to show the gain in performance because of the multiple widely separated antennas. For the SISO system, we consider only the first transmit and receive antennas in our above mentioned example. Therefore, the covariance matrix of the scattering vector $\boldsymbol{s}$ becomes $\boldsymbol{\Sigma}_{\boldsymbol{s}} = \boldsymbol{\Sigma}_{\boldsymbol{s}}^{11}$. In order to make a fair comparison, we transmit more power than the power transmitted

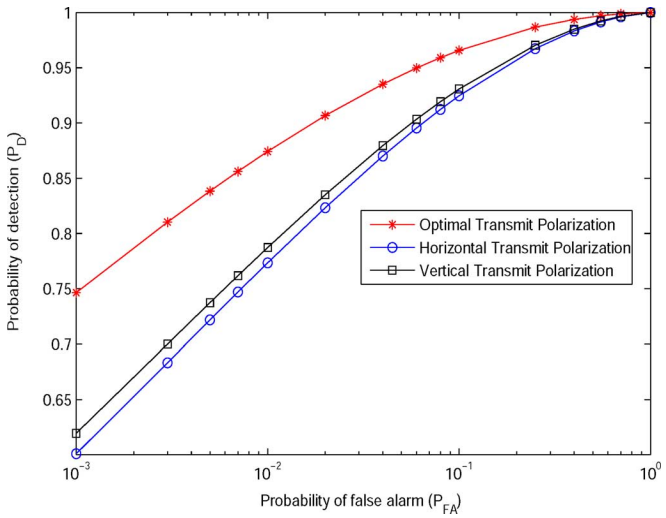

Fig. 3. ROC curves demonstrating the improvement offered by the optimal choice of polarizations when $\sigma^2 = 0.2$.

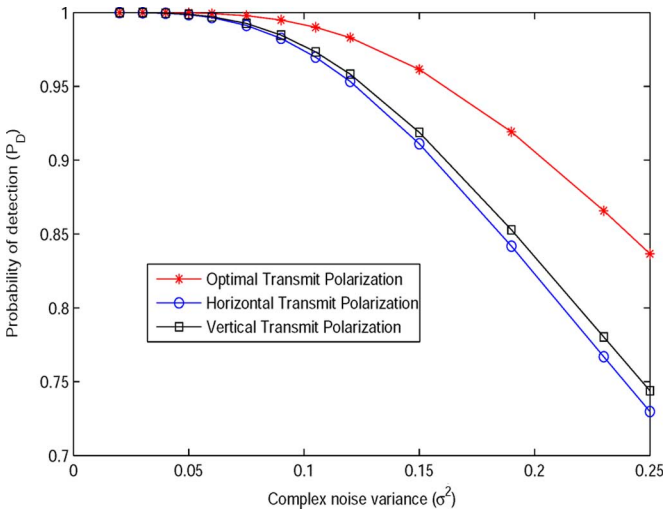

Fig. 4. Probability of detection (P_{D}) as a function of the complex noise variance when $P_{\mathrm{FA}} = 0.02$.

per antenna while using MIMO radar. It is clear from Fig. 5 that 2×2 polarimetric MIMO radar system significantly outperforms its SISO counterpart even when the SISO system uses four times the transmit power used by each antenna in the 2×2 system.

The complexity of the grid search for optimization using our proposed system model does not increase much with the increase in the number of receivers, because the number of variables over which the optimization is performed depends only on the number of transmit antennas. However, with the scalar measurement model, the addition of each extra receiver adds extra variables (receive polarization vectors) in the grid search and makes the calculations more complex. Therefore, in order to compare the performance of our proposed system with that of the scalar measurement system, we use the same numerical example as described so far; however, this time we stick to just two transmitters and one receiver to reduce the complexity of the optimization step. The $\boldsymbol{\Sigma_s}$ matrix now has the following form:

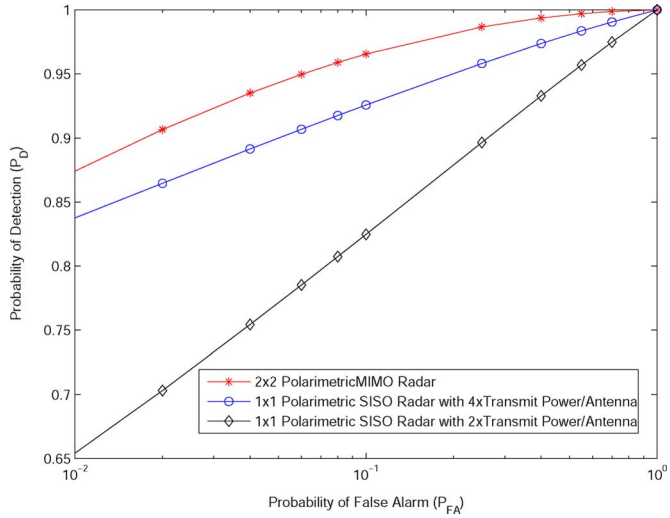

Fig. 5. ROC curves demonstrating the improvement offered by employing multiple widely separated antennas compared with single input single output systems when $\sigma^2 = 0.2$.

$$\boldsymbol{\Sigma_s} = \begin{bmatrix} \boldsymbol{\Sigma_s^{11}} & \mathbf{0} \\ \mathbf{0} & \boldsymbol{\Sigma_s^{21}} \end{bmatrix} \tag{37}$$

where matrices $\boldsymbol{\Sigma_s^{11}}$ and $\boldsymbol{\Sigma_s^{21}}$ are chosen to be the same, as defined earlier in this section. The noise variance remains the same for both the systems because the receive polarization vectors are assumed to be unit norm. We assume the same noise variance $\sigma^2 = 0.1$ for both systems in order to make a fair comparison. Fig. 6 compares the performance of both systems under the optimal choice of polarization vectors. It clearly shows that by retaining the 2-D vector measurements, we get significantly improved results as compared with scalar measurement systems. Even though we perform joint optimization over both the transmit and receive polarizations for the scalar measurement systems, we are still finding just the best linear combination of the two received measurements at each receiver. However, combining them linearly need not be the overall optimal solution and we might be losing some important information by doing so. This can be avoided by retaining the vector measurements, thereby giving better performance as demonstrated in Fig. 6.

Fig. 7 shows the performance of both systems as a function of the noise variance when P_{FA} is fixed to a constant value of 0.02. At higher noise variances (lower signal-to-noise ratios), the improvement offered by retaining the 2-D vector measurements becomes even more evident.

VII. Conclusion

We have proposed a radar system that combines the advantages of MIMO radar with distributed antennas and polarimetric radar at the same time. The proposed system uses 2-D vector sensors at each of the receivers, measuring both the horizontal and vertical components of the received signal. We dealt with the problem of target detection for such a system. We designed the well-known Neyman–Pearson detector for this problem and also analyzed the performance of the detector by obtaining approximate expressions for the probabilities of false alarm and detection. We developed a similar mathematical model for the

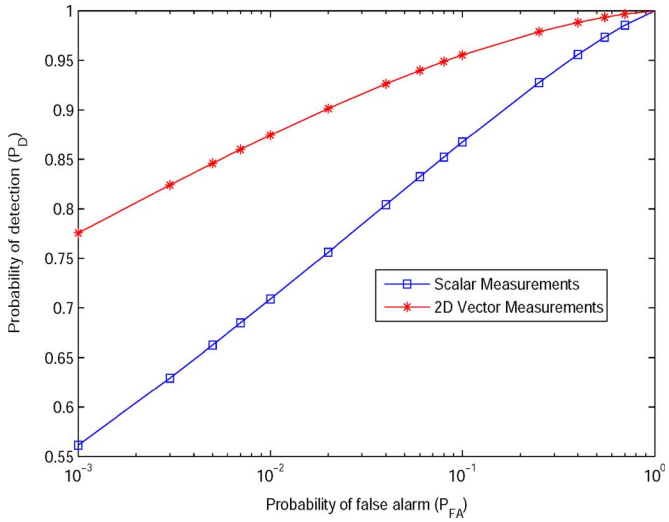

Fig. 6. Comparison of performance between systems with scalar measurements and those with 2-D vector measurements as a function of the probability of false alarm when $\sigma^2 = 0.1$.

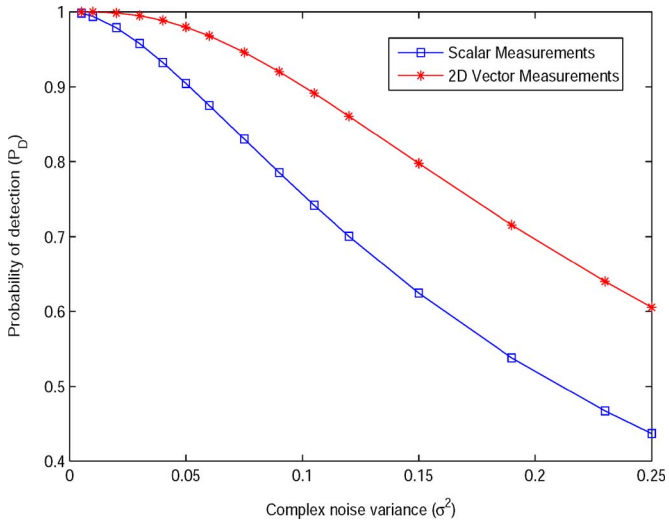

Fig. 7. Comparison of performance between systems with scalar measurements and those with 2-D vector measurements as a function of the noise variance when $P_{\mathrm{FA}} = 0.02$.

conventional systems that combine the two received signals linearly and coherently to give only a scalar measurement at the receiver. Using numerical examples, we showed that the optimal selection of the polarizations gives significant improvement in performance over conventional systems using only horizontal or vertical polarizations all the time across all the antennas. We showed that the performance improves by employing multiple widely separated antennas. We also demonstrated that retaining the 2-D vector measurements enhances the performance of the proposed polarimetric MIMO radar system, especially at low signal-to-noise ratios.

REFERENCES

[1] W. M. Boerner, W. L. Yan, A. Q. Xi, and Y. Yamaguchi, "On the basic principles of radar polarimetry: The target characteristic polarization state theory of Kennaugh, Huynen's polarization fork concept, and its extension to the partially polarized case," *Proc. IEEE*, vol. 79, no. 10, pp. 1538–1550, Oct. 1991.

[2] D. Giuli, "Polarization diversity in radars," *Proc. IEEE*, vol. 74, no. 2, pp. 245–269, Feb. 1986.

[3] M. Hurtado, J. J. Xiao, and A. Nehorai, "Target estimation, detection, and tracking: A look at adaptive polarimetric design," *IEEE Signal Process. Mag.*, vol. 26, no. 1, pp. 42–52, Jan. 2009.

[4] D. Pastina, P. Lombardo, and T. Bucciarelli, "Adaptive polarimetric target detection with coherent radar. I. Detection against Gaussian background," *IEEE Trans. Aerosp. Electron. Syst.*, vol. 37, no. 10, pp. 1194–1206, Oct. 2001.

[5] P. Lombardo, D. Pastina, and T. Bucciarelli, "Adaptive polarimetric target detection with coherent radar. II. Detection against non-Gaussian background," *IEEE Trans. Aerosp. Electron. Syst.*, vol. 37, no. 10, pp. 1207–1220, Oct. 2001.

[6] J. Wang and A. Nehorai, "Adaptive polarimetry design for a target in compound-Gaussian clutter," presented at the Int. Waveform Diversity Des. (WDD) Conf., Lihue, HI, Jan. 2006.

[7] L. M. Novak, M. B. Sechtin, and M. J. Cardullo, "Studies of target detection algorithms that use polarimetric radar data," *IEEE Trans. Aerosp. Electron. Syst.*, vol. AES-25, no. 2, pp. 150–165, Mar. 1989.

[8] A. R. Calderbank, S. D. Howard, W. Moran, A. Pezeshki, and M. Zoltowski, "Instantaneous radar polarimetry with multiple dually-polarized antennas," presented at the 40th Asilomar Conf. Signals, Syst. Comput., Pacific Grove, CA, Oct. 2006.

[9] M. I. Skolnik, *Introduction to Radar Systems*. New York: McGraw-Hill, 2001.

[10] A. M. Haimovich, R. S. Blum, and L. J. Cimini, "MIMO radar with widely separated antennas," *IEEE Signal Process. Mag.*, vol. 25, no. 1, pp. 116–129, Jan. 2008.

[11] J. Li and P. Stoica, *MIMO Radar Signal Processing*. Hoboken, NJ: Wiley, 2009.

[12] J. Li and P. Stoica, "MIMO radar with colocated antennas," *IEEE Signal Process. Mag.*, vol. 24, pp. 106–114, Sep. 2007.

[13] J. Li, P. Stoica, L. Xu, and W. Roberts, "On parameter identifiability of MIMO radar," *IEEE Signal Process. Lett.*, vol. 14, no. 12, pp. 968–971, Dec. 2007.

[14] M. Akcakaya, M. Hurtado, and A. Nehorai, "MIMO radar detection of targets in compound-gaussian clutter," in *Proc. 42nd Asilomar Conf. Signals, Syst. Comput.*, 2008, pp. 208–212.

[15] J. Zhang, B. Manjunath, G. Maalouli, A. Papandreou-Suppappola, and D. Morrell, "Dynamic waveform design for target tracking using MIMO radar," in *Proc. 42nd Asilomar Conf. Signals, Syst. Comput.*, pp. 31–35.

[16] A. Hassanien and S. A. Vorobyov, "Transmit/receive beamforming for MIMO radar with colocated antennas," in *Proc. IEEE Int. Conf. Acoust., Speech Signal Process.*, 2009, pp. 2089–2092.

[17] J. J. Zhang and A. Papandreou-Suppappola, "MIMO radar with frequency diversity," in *Proc. Int. Waveform Diversity Des. (WDD) Conf.*, 2009, pp. 208–212.

[18] A. Nehorai and E. Paldi, "Vector-sensor array processing for electromagnetic source localization," *IEEE Trans. Signal Process.*, vol. 42, no. 2, pp. 376–398, Feb. 1994.

[19] A. Nehorai and E. Paldi, "Acoustic vector-sensor array processing," *IEEE Trans. Signal Process.*, vol. 42, no. 9, pp. 2481–2491, Sep. 1994.

[20] J.-J. Xiao and A. Nehorai, "Joint transmitter and receiver polarization optimization for scattering estimation in clutter," *IEEE Trans. Signal Process.*, vol. 57, no. 10, pp. 4142–4147, Oct. 2009.

[21] R. Touzi, W. M. Boerner, J. S. Lee, and E. Lueneburg, "A review of polarimetry in the context of synthetic aperture radar: Concepts and information extraction," *Can. J. Remote Sens.*, vol. 30, no. 3, pp. 380–407, 2004.

[22] M. Hurtado and A. Nehorai, "Polarimetric detection of targets in heavy inhomogeneous clutter," *IEEE Trans. Signal Process.*, vol. 56, no. 4, pp. 1349–1361, Apr. 2008.

[23] J. A. Gubner, *Probability and Random Processes for Electrical and Computer Engineers*. New York: Cambridge University Press, 2006.

[24] L. L. Scharf, *Statistical Signal Processing: Detection, Estimation, and Time Series Analysis*. Reading, MA: Addison-Wesley, 1991.

[25] E. J. Kelly, "An adaptive detection algorithm," *IEEE Trans. Aerosp. Electron. Syst.*, vol. 22, no. 2, pp. 115–127, Mar. 1986.

[26] S. R. Searle, *Linear Models*. New York: Wiley, 1971.

[27] A. H. Feiveson and F. C. Delaney, "The distribution and properties of a weighted sum of Chi squares," *NASA Techn. Note*, May 1968.

[28] S. M. Kay, *Fundamentals of Statistical Signal Processing: Detection Theory*. Englewood Cliffs, NJ: Prentice-Hall, Inc., 1998.

Sandeep Gogineni (S'08) received the B.Tech. degree in electronics and communications engineering (with Honors in signal processing and communications) from International Institute of Information Technology, Hyderabad, India, in 2007. He is currently pursuing the Ph.D. degree from the Department of Electrical and Systems Engineering, Washington University, St. Louis, MO.

His research interests include statistical signal processing, radar, and communications systems.

Arye Nehorai (S'80–M'83–SM'90–F'94) received the B.Sc. and M.Sc. degrees in electrical engineering from the Technion-Israeli Institute of Technology, Haifa, Israel, and the Ph.D. degree in electrical engineering from Stanford University, Stanford, CA.

From 1985 to 1995 he was a faculty member with the Department of Electrical Engineering, Yale University. In 1995, he was a Full Professor with the Department of Electrical Engineering and Computer Science, The University of Illinois at Chicago (UIC). From 2000 to 2001, he was Chair of the department's Electrical and Computer Engineering (ECE) Division, which then became a new department. In 2001, he was named University Scholar of the University of Illinois. In 2006, he became Chairman of the Department of Electrical and Systems Engineering at Washington University in St. Louis. He is the inaugural holder of the Eugene and Martha Lohman Professorship and the Director of the Center for Sensor Signal and Information Processing (CSSIP) at WUSTL since 2006.

Dr. Nehorai was Editor-in-Chief of the IEEE TRANSACTIONS ON SIGNAL PROCESSING during the years 2000 to 2002. From 2003 to 2005, he was Vice President (Publications) of the IEEE Signal Processing Society, Chair of the Publications Board, member of the Board of Governors, and member of the Executive Committee of this Society. From 2003 to 2006, he was the founding editor of the special columns on Leadership Reflections in the IEEE SIGNAL PROCESSING MAGAZINE. He was a corecipient of the IEEE SPS 1989 Senior Award for Best Paper with P. Stoica, coauthor of the 2003 Young Author Best Paper Award, and corecipient of the 2004 Magazine Paper Award with A. Dogandzic. He was elected Distinguished Lecturer of the IEEE SPS for the term 2004 to 2005 and received the 2006 IEEE SPS Technical Achievement Award. He is the Principal Investigator of the new multidisciplinary university research initiative (MURI) project entitled Adaptive Waveform Diversity for Full Spectral Dominance. He has been a Fellow of the Royal Statistical Society since 1996.